Formations of Vehicles in Cyclic Pursuit

Joshua A. Marshall, *Student Member, IEEE*, Mireille E. Broucke, *Member, IEEE*, and Bruce A. Francis, *Fellow, IEEE*

***Abstract*—Inspired by the so-called "bugs" problem from mathematics, we study the geometric formations of multivehicle systems under cyclic pursuit. First, we introduce the notion of cyclic pursuit by examining a system of identical linear agents in the plane. This idea is then extended to a system of wheeled vehicles, each subject to a single nonholonomic constraint (i.e., unicycles), which is the principal focus of this paper. The pursuit framework is particularly simple in that the n identical vehicles are ordered such that vehicle i pursues vehicle $i+1$ modulo n. In this paper, we assume each vehicle has the same constant forward speed. We show that the system's equilibrium formations are generalized regular polygons and it is exposed how the multivehicle system's global behavior can be shaped through appropriate controller gain assignments. We then study the local stability of these equilibrium polygons, revealing which formations are stable and which are not.**

***Index Terms*—Circulant matrices, cooperative control, multiagent systems, pursuit problems.**

I. Introduction

THIS PAPER proposes a reconfiguration strategy for multivehicle systems based on the notion of *cyclic pursuit* from mathematics. Multiagent systems might find application in terrestrial, space, and oceanic exploration [1], military surveillance and rescue missions, or even automated highway systems [2], [3]. Hence, from an engineering standpoint, the question of how to prescribe desired *global* behaviors through the application of only simple and *local* interactions is of significant and practical interest.

On this subject, perhaps the most famous artificially created example is the distributed behavioral model of Reynolds [4]. Reynolds' so-called *boids* (or bird-oids) each obey a set of local interaction rules, which together result in a natural and appealing steady-state flocking behavior for the group. In fact, much of the multiagent robotics research has focused on the use of similar reactive or *behavior-based* techniques. For example, Balch and Arkin [5] evaluated reactive behaviors designed to implement multivehicle formations in combination with rules for collision avoidance and other navigational goals. Not unlike Reynolds' boids, the behavior-based approach is often to mimic biological systems, where self-organizing or emergent behaviors result from agents that appear to act autonomously. For a more complete review, see [1], [6], [7], and the references therein.

However, the global outcome of these behavior-based systems is often difficult to predict analytically. Thus, corresponding mathematical results are rare, as noted in [7] and [8]. Some have argued that rigorous analysis of even the most simple cases can be an impractical task [9]. On the other hand, this has not deterred interest in analyzing "nearest-neighbor" strategies, where simple navigational rules are employed locally to generate global formations. For example, Wang [10] proposed a strategy where agents are instructed to move based on the motions of their nearest neighbors. Certain formation stability properties were then analyzed for the case when one agent is provided a reference trajectory and designated group leader. Early work by Sugihara and Suzuki [8] investigated a set of heuristic algorithms for the generation of geometric patterns in the plane (e.g., lines, circles, or polygons). More recent work has stressed the need for rigorous proof of the correctness of these types of algorithms [11]. Very recently, Justh and Krishnaprasad [12], [13] have developed steering laws for achieving both rectilinear and circular formations in the plane. In their approach, each vehicle's control input, which is based on the pose of all other vehicles in the group, uses alignment and separation terms to determine the formation. Jadbabaie *et al.* [14] proved convergence results for a nearest-neighbor type problem, guaranteeing that all agents eventually move in an identical fashion, despite the distributed nature of the coordination law.

Indeed, patterns of this sort seem to appear in nature. For example, Bruckstein's curiosity with regards to the evolution of ant trails led him to an interesting mathematical discovery in [15]. Others have studied aggregate behavior in *swarms* of organizms (e.g., birds, fish, mammals, and bacteria), where operational models are analyzed for the purpose of potential engineering application (e.g., see [16], [17], and the references therein). Still, many of these distributed coordination ideas have yet to be explored for agents subject to motion constraints, such as wheeled vehicles.

Inspired by the so-called "bugs" problem from mathematics, in this paper we study the geometric formations of multivehicle systems under cyclic pursuit. The bugs problem refers to what is also variously known as the dogs, mice, ants, or beetles problem, and originally stems from the mathematics of *pursuit curves*, first studied by French scientist Pierre Bouguer (c. 1732). In 1877, Edouard Lucas asked, what trajectories would be generated if three dogs, initially placed at the vertices of an equilateral triangle, were to run one after the other? Three years later, Henri Brocard replied with the answer that each dog's pursuit curve would be that of a logarithmic spiral and that the dogs would meet at a common point, known now as the *Brocard point* of a triangle. Bernhart [18] reports that Gordon Peterson extended this problem to n ordered bugs that start at the vertices of a regular n-polygon, illustrating his results for the square using four "cannibalistic spiders." If each bug pursues the next modulo n (i.e., *cyclic* pursuit) at fixed speed, the bugs will trace out logarithmic spirals and eventually meet at

Manuscript received September 30, 2003; revised April 13, 2004. Recommended by Associate Editor A. Garulli. This work was supported in part by the Natural Sciences and Engineering Research Council of Canada (NSERC).

The authors are with the Department of Electrical and Computer Engineering, Systems Control Group, University of Toronto, Toronto, ON M5S 3G4, Canada (e-mail: marshall@control.toronto.edu; broucke@control.toronto.edu; francis@control.toronto.edu).

Digital Object Identifier 10.1109/TAC.2004.837589

the polygon's centre. In 1969, Watton and Kydon [19] provided an elegant solution to this regular n-bugs problem, further noting that the constant-speed assumption taken by previous investigators is not necessary.

What happens if our n bugs do not start at the vertices of a regular n-polygon? In 1971, Klamkin and Newman [20] showed that, for three bugs, so long as the initial triangle formed by the bugs is not degenerate (i.e., the bugs are not collinear), they will meet at a point and this meeting will be mutual. For n bugs, this notion was later examined by Behroozi and Gagnon [21], who proved that "a bug cannot capture a bug which is not capturing another bug (i.e., *mutual* capture), except by head-on collision." They used this result to show that, for the general four-bugs problem, the capture is indeed mutual. Quite recently, Richardson [22] resolved this issue for the general n-bugs problem, showing that "it is possible for bugs to capture their prey without all bugs simultaneously doing so, even for noncollinear initial positions." However, he proved that for randomly chosen initial positions, the probability of a nonmutual capture is exactly zero. For a more complete historical review of cyclic pursuit, see [18], [22], and the references therein.

Variations on this traditional cyclic pursuit problem have also been studied. For example, Bruckstein *et al.* [23] investigated both continuous and discrete pursuit problems, as well as both constant and varying speed scenarios.

Consider now a particular cyclic pursuit scheme where each "bug" is additionally subject to a single nonholonomic constraint, or equivalently, modeled as a kinematic unicycle. In this case, the unicycles will not generally be able to head toward their designated prey at each instant. Instead, depending on the allowed control energy, each vehicle will require some finite time to steer itself toward its preassigned target. What trajectories can be generated? We first asked this question in [24]. In this paper, we generalize the cyclic pursuit concept to nonholonomic vehicles and study its properties as a coordination algorithm for multivehicle systems. Thus, our primary motivation is to follow historical development and study the achievable formations for wheeled vehicles under cyclic pursuit. On the other hand, from a practical viewpoint, cyclic pursuit may turn out to be a feasible strategy for multivehicle systems since it is distributed (i.e., decentralized and there is no leader) and relatively simple in that each agent is required to sense information from only one other agent.

A growing number of researchers in the field of multiagent systems have come to realize that algebraic graph theory might serve as an effective tool for modeling interagent connectivity [14], [25]. In the case of cyclic pursuit, it is clear that the graph representing agent interconnections is cyclic in nature.

Our analysis begins by examining a linear version of the n-bugs problem, mainly as a means for introducing our chosen mathematical framework. These ideas are then extended to a system of n wheeled vehicles, which is the principal focus of this paper. We study one particular control law, which assumes that each vehicle has the same constant forward speed, unlike in [24]. We show that the multivehicle system's equilibrium formations are generalized regular polygons and it is exposed how the system's global behavior can be shaped by appropriate controller gain assignments. Then, we study the local stability of these equilibrium polygons, revealing which formations are stable and which are not.

II. Mathematical Preliminaries

We assume the reader is familiar with certain standard results from linear and nonlinear systems theory, as well as with some basic concepts from differential geometry. In this section, we summarize some results from the theory of circulant matrices, which are fundamental to our approach. For a detailed treatise, the reader is referred to the authoritative text by Davis [26].

A. Circulant Matrices

A *circulant matrix* (or *circulant* for short) of order n is a square matrix of the form

$$C = \begin{bmatrix} c_1 & c_2 & \cdots & c_n \\ c_n & c_1 & \cdots & c_{n-1} \\ \vdots & \vdots & & \vdots \\ c_2 & c_3 & \cdots & c_1 \end{bmatrix} =: \operatorname{circ}[c_1, c_2, \ldots, c_n].$$

Each subsequent row is simply the row above shifted one element to the right (and wrapped around, i.e., modulo n). The entire matrix is determined by the first row.

Let Π_n denote the special $n \times n$ permutation matrix

$$\Pi_n = \begin{bmatrix} 0 & 1 & 0 & 0 & \cdots & 0 \\ 0 & 0 & 1 & 0 & \cdots & 0 \\ \vdots & \vdots & \vdots & \vdots & & \vdots \\ 1 & 0 & 0 & 0 & \cdots & 0 \end{bmatrix}$$

which plays a fundamental role in the theory of circulants. One can then "push forward" the matrix Π_n to form subsequent permutation matrices; for example

$$\Pi_n^2 = \begin{bmatrix} 0 & 0 & 1 & 0 & \cdots & 0 \\ 0 & 0 & 0 & 1 & \cdots & 0 \\ \vdots & \vdots & \vdots & \vdots & & \vdots \\ 0 & 1 & 0 & 0 & \cdots & 0 \end{bmatrix}$$

and subsequently $\Pi_n^3, \Pi_n^4, \ldots$, and so on. Note that Π_n is itself circulant. Let $I_n = \Pi_n^0$ denote the $n \times n$ identity matrix. Using the structure of the permutation matrices Π_n^k, with $k = 0, 1, \ldots, n-1$, every circulant C can be represented by

$$\begin{aligned} C &= \operatorname{circ}[c_1, c_2, \ldots, c_n] \\ &= c_1 I_n + c_2 \Pi_n + c_3 \Pi_n^2 + \cdots + c_n \Pi_n^{n-1}. \end{aligned}$$

Thus, the polynomial $p_C(\lambda) = c_1 + c_2\lambda + c_3\lambda^2 + \cdots + c_n\lambda^{n-1}$ is called the circulant's *representer*, since $C = p_C(\Pi_n)$.

B. Diagonalization of Circulants

Define $\omega := e^{2\pi j/n}$ where $j = \sqrt{-1}$ and let $\Omega_n = \operatorname{diag}[1, \omega, \omega^2, \ldots, \omega^{n-1}]$, which are the n roots of unity. Let F_n denote the $n \times n$ *Fourier matrix* given via

$$F_n^* = \frac{1}{\sqrt{n}} \begin{bmatrix} 1 & 1 & 1 & \cdots & 1 \\ 1 & \omega & \omega^2 & \cdots & \omega^{n-1} \\ 1 & \omega^2 & \omega^4 & \cdots & \omega^{2(n-1)} \\ \vdots & \vdots & \vdots & & \vdots \\ 1 & \omega^{n-1} & \omega^{2(n-1)} & \cdots & \omega^{(n-1)(n-1)} \end{bmatrix}$$

and note that $F_n^* = (F_n^*)^\top$ and so $F_n = F_n^\top$. Also, $F_n F_n^* = I_n$ (i.e., it is unitary). It is possible to verify the following diagonalization formula for Π_n.

Theorem 1 [26, Th. 3.2.1]: $\Pi_n = F_n^* \Omega_n F_n$. Then, we have the following.

Theorem 2 (After [26, Th. 3.2.2.]): If C is an $n \times n$ circulant matrix, then it is diagonalizable by the Fourier matrix F_n. More precisely, the circulant $C = F_n^* \Lambda_C F_n$, where $\Lambda_C = \mathrm{diag}(p_C(1), p_C(\omega), \ldots, p_C(\omega^{n-1}))$.

Corollary 1: The eigenvalues of C are $\lambda_i = p_C(\omega^{i-1})$, where $i = 1, 2, \ldots, n$.

C. Block Circulant Matrices

First, we recall the Kronecker product. Let A and B be $m \times n$ and $p \times q$ matrices, respectively. Then, the *Kronecker product* of A and B is the $mp \times nq$ matrix

$$A \otimes B := \begin{bmatrix} a_{11}B & \cdots & a_{1n}B \\ \vdots & & \vdots \\ a_{m1}B & \cdots & a_{mn}B \end{bmatrix}$$

where a_{ij} are the elements of A, $i \in \{1, 2, \ldots, m\}$ and $j \in \{1, 2, \ldots, n\}$. A useful property of the Kronecker product is that $AC \otimes BD = (A \otimes B)(C \otimes D)$.

Let $A_1, A_2, \ldots, A_n$ be $m \times m$ matrices. A *block circulant* matrix of type (m, n) is a $mn \times mn$ matrix[1] of the form

$$A = \begin{bmatrix} A_1 & A_2 & \cdots & A_n \\ A_n & A_1 & \cdots & A_{n-1} \\ \vdots & \vdots & & \vdots \\ A_2 & A_3 & \cdots & A_1 \end{bmatrix} =: \mathrm{circ}[A_1, A_2, \ldots, A_n].$$

Note that A is not necessarily circulant (only *block* circulant). We designate the set of block circulant matrices of type (m, n) by $\mathcal{BC}(m, n)$. Similar to circulant matrices, every block circulant A can be represented by

$$A = \mathrm{circ}[A_1, A_2, \ldots, A_n] = \sum_{k=0}^{n-1} \left(\Pi_n^k \otimes A_{k+1}\right).$$

Theorem 3 (Adapted From [26, Th. 5.6.4]): If $A \in \mathcal{BC}(m, n)$, then it has the form

$$A = (F_n \otimes I_m)^* \mathrm{diag}(D_1, D_2, \ldots, D_n)(F_n \otimes I_m)$$

where the D_i blocks are given via

$$\begin{bmatrix} D_1 \\ D_2 \\ \vdots \\ D_n \end{bmatrix} = \left(\sqrt{n} F_n^* \otimes I_m\right) \begin{bmatrix} A_1 \\ A_2 \\ \vdots \\ A_n \end{bmatrix}.$$

Theorem 3 gives us a way to block diagonalize block circulant matrices. Using the fact that $(F_n \otimes I_m)^*(F_n \otimes I_m) = I_{mn}$, we get that

$$\Lambda_M = \mathrm{diag}(D_1, D_2, \ldots, D_n) = (F_n \otimes I_m) A (F_n \otimes I_m)^*.$$

[1]Our notation differs slightly from that of Davis [26].

III. Linear Cyclic Pursuit

We begin by revisiting the classical n-bugs problem, but formalized using a simple differential equation model for each agent, as in [23] and [27]. Let there be n ordered mobile agents in the plane, their positions at time $t \geq 0$ denoted $z_i(t) = [x_i(t), y_i(t)]^\top \in \mathbb{R}^2$, $i = 1, 2, \ldots, n$, where agent i pursues the next $i + 1$ modulo[2] n.

Suppose the agents start with *arbitrary* initial conditions and that the kinematics of each agent are described by an integrator

$$\dot{z}_i = u_i \tag{1}$$

with control inputs

$$u_i = k\,(z_{i+1} - z_i) \tag{2}$$

for some positive constant k. Thus, the velocity of agent i is simply proportional to the vector from agent i to its prey, agent $i + 1$. Since each coordinate of z_i evolves independently, the planar linear n-agent system (1)–(2) decouples into two identical linear systems of the form

$$\dot{x} = Ax \tag{3}$$

where $x = [x_1, x_2, \ldots, x_n]^\top \in \mathbb{R}^n$ and the matrix $A = \mathrm{circ}[-k, k, 0, \ldots, 0]$ is circulant.

Bruckstein *et al.* [23] proved that for every initial condition, these agents exponentially converge to a single limit point. Moreover, they showed that this limit point is computable from the initial positions of the agents. Another version of the following theorem can also be found in [27].

Theorem 4: Consider n planar agents with kinematics(1)–(2). For every initial condition, the centroid of the agents $z_1(t), z_2(t), \ldots, z_n(t)$ remains stationary and every agent $z_i(t)$, $i = 1, 2, \ldots, n$ exponentially converges to this centroid.

As a preview of our extension to kinematic unicycles, we provide a proof that differs from those of [23], [27]. Our proof may not be as efficient, but serves to introduce a certain perspective that will later prove useful.

Proof of Theorem 4: As previously noted, we need only study the linear system (3). From the circulant structure of A, this system's equilibrium point $\bar{x} = [\bar{x}_1, \bar{x}_2, \ldots, \bar{x}_n]^\top$ must satisfy $\bar{x}_1 = \bar{x}_2 = \cdots = \bar{x}_n$. Moreover, due to *cyclic* pursuit

$$\sum_{i=1}^{n} \dot{x}_i(t) = 0 \Longrightarrow \sum_{i=1}^{n} x_i(t) \equiv c, \qquad \text{for all } t \geq 0 \tag{4}$$

where the constant c is determined by the set of initial locations via $c = \sum_{i=1}^{n} x_i(0)$. In other words, the equilibrium point $\bar{x}$ must be the centroid; that is $\bar{x}_i = 1/n \sum_{i=1}^{n} x_i(0)$. The centroid is also stationary by (4). We can choose $c = 0$ without loss of generality.

Therefore, for every initial condition, system (3) is constrained to evolve on the A-invariant subspace $\mathcal{S} \subset \mathbb{R}^n$ defined by $\mathcal{S} = \{x \in \mathbb{R}^n : [1 \quad 1 \quad \cdots \quad 1]\, x = 0\}$. The subspace $\mathcal{S}$ is clearly A-invariant, since every column of A is an element

[2]Henceforth, all agent/vehicle indices $i + 1$ should be evaluated modulo n.

of $\mathcal{S}$. Because $\mathcal{S}$ is A-invariant, there exists an induced linear transformation in the quotient space $A^{\star}_{\mathcal{S}} : \mathbb{R}^n/\mathcal{S} \to \mathbb{R}^n/\mathcal{S}$ whose eigenvalues do not influence the stability of the point $\bar{x} \in \mathcal{S}$. Therefore, there exists a change of basis that transforms A into upper triangular form

$$\begin{bmatrix} A_{\mathcal{S}} & * \\ 0_{1\times(n-1)} & A^{\star}_{\mathcal{S}} \end{bmatrix}.$$

Consider the change of coordinates $\tilde{x} = Px$ such that

$$\tilde{x}_1 = x_1, \tilde{x}_2 = x_2, \ldots, \tilde{x}_{n-1} = x_{n-1}, \tilde{x}_n = \sum_{i=1}^{n} x_i$$

which, by explicit computations not shown, gives

$$\dot{\tilde{x}} = \left[\begin{array}{ccccc|c} -k & k & 0 & \cdots & \cdots & 0 \\ 0 & -k & k & 0 & \cdots & 0 \\ 0 & 0 & \ddots & \ddots & 0 & 0 \\ 0 & \cdots & 0 & -k & k & 0 \\ -k & \cdots & \cdots & -k & -2k & k \\ \hline 0 & \cdots & \cdots & \cdots & 0 & 0 \end{array}\right] \tilde{x} = \begin{bmatrix} A_{\mathcal{S}} & * \\ 0_{1\times(n-1)} & A^{\star}_{\mathcal{S}} \end{bmatrix} \tilde{x}.$$

Therefore, when determining the stability of $\bar{x}$ we can disregard exactly one zero eigenvalue and conclude stability based on the remaining $n-1$ eigenvalues of A.

The matrix A is circulant. Thus, the representer of A is $p_A(\lambda) = k(\lambda - 1)$. So, by Corollary 1, the eigenvalues of A must be given by $\lambda_i = p_A(\omega^{i-1})$; that is

$$\lambda_i = k\left[\cos\left(\frac{2\pi(i-1)}{n}\right) - 1\right] + jk\sin\left(\frac{2\pi(i-1)}{n}\right)$$

with $i = 1, 2, \ldots, n$. Thus, for all $k > 0$, A always has exactly one zero eigenvalue, while the remaining $n-1$ eigenvalues lie strictly in the left-half complex plane. ■

IV. Nonlinear Equations of Pursuit

The linear pursuit problem is in itself quite interesting and it has some beautiful extensions (e.g., see [27]). However, the focus of this paper is on a nonlinear analog involving wheeled vehicles, each subject to a single nonholonomic constraint.

Suppose we extend the aforementioned linear cyclic pursuit scenario to one in which each agent is a kinematic unicycle with nonlinear state model

$$\begin{bmatrix} \dot{x}_i \\ \dot{y}_i \\ \dot{\theta}_i \end{bmatrix} = \begin{bmatrix} \cos\theta_i & 0 \\ \sin\theta_i & 0 \\ 0 & 1 \end{bmatrix} \begin{bmatrix} v_i \\ \omega_i \end{bmatrix} = G(\theta_i)u_i \tag{5}$$

where $[x_i, y_i]^{\top} \in \mathbb{R}^2$ denotes the i-th vehicle's position, $\theta_i \in \mathbb{R}$ is the vehicle's orientation, and $u_i = [v_i, \omega_i]^{\top} \in \mathbb{R}^2$ are control inputs. In this paper, we allow angles to take values in the set $\mathbb{R}$ to avoid a discontinuity in our feedback law, which depends on angles.

Let r_i denote the distance between vehicle i and $i+1$, and let α_i be the difference between the ith vehicle's heading and the heading that would take it directly toward its prey, $i+1$ (see Fig. 1). In analogy with the linear controls (2), and as we proposed in [24], an intuitive pursuit law for (5) is to assign vehicle i's forward speed v_i in proportion to the distance error r_i, while assigning its angular speed ω_i in proportion to the heading error α_i. In this paper, we fix each vehicle's forward speed and study the possible equilibrium formations for multivehicle systems of this sort.

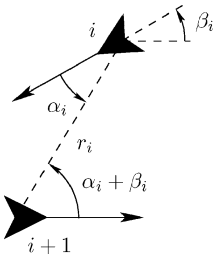

Fig. 1. New coordinates with vehicle i in pursuit of $i+1$.

A. Transformation to Relative Coordinates

In addition to r_i and α_i, define the angle β_i as in Fig. 1. After some (rather tedious) algebraic manipulation, the kinematic equations become

$$\dot{r}_i = -v_i\cos\alpha_i - v_{i+1}\cos(\alpha_i + \beta_i) \tag{6a}$$

$$\dot{\alpha}_i = \frac{1}{r_i}\left[v_i\sin\alpha_i + v_{i+1}\sin(\alpha_i + \beta_i)\right] - \omega_i \tag{6b}$$

$$\dot{\beta}_i = \omega_i - \omega_{i+1}. \tag{6c}$$

This system describes the relationship between vehicle i and the one that it is pursuing, $i+1$. Note that, in these coordinates, it is assumed that $r_i > 0$. One might also observe that the transformation from q_i into $\xi_i = [r_i, \alpha_i, \beta_i]^{\top}$ is not invertible, which is not surprising since we have removed any reference to a global coordinate frame. This transformation to relative coordinates implies the existence of constraints on the system, as described in the next subsection.

B. Formation Control and Pursuit Graph

As previously suggested, we investigate the case when

$$v_i = s \text{ and } \omega_i = k\alpha_i \tag{7}$$

where $k, s > 0$ are constant. Substituting these controls into (6) gives a system of n cyclically interconnected and identical nonlinear subsystems of the form

$$\dot{r}_i = -s\left[\cos\alpha_i + \cos(\alpha_i + \beta_i)\right] \tag{8a}$$

$$\dot{\alpha}_i = \frac{s}{r_i}\left[\sin\alpha_i + \sin(\alpha_i + \beta_i)\right] - k\alpha_i \tag{8b}$$

$$\dot{\beta}_i = k(\alpha_i - \alpha_{i+1}). \tag{8c}$$

At each instant in time, regardless of the control law, the multivehicle system's geometric configuration in the plane can be described by a *pursuit graph* as follows.

Definition 1 (Pursuit Graph): A *pursuit graph* G consists of a pair (V, E) such that

1) V is a finite set of vertices, $|V| = n$, where each vertex $z_i = (x_i, y_i) \in \mathbb{R}^2$, $i \in \{1, 2, \ldots, n\}$, represents the position of vehicle i in the plane;

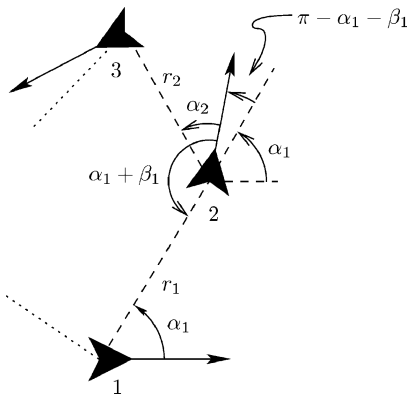

Fig. 2. Depiction of coordinates for vehicles 1 and 2.

2) E is a finite set of directed edges, $|E| = n$, where each edge $e_i : V \times V \to \mathbb{R}^2$, $i \in \{1, 2, \ldots, n\}$, is the vector from z_i to its prey, z_{i+1}.

Although not stated explicitly in the previous definition, for the purposes of this paper we view two pursuit graphs as being equivalent if there exists a rotation and/or translation such that vertices are mapped to vertices and edges mapped to edges with the sense of directions preserved.

This definition is employed in characterizing the equilibrium formations of our multivehicle system. Note that the coordinate $r_i \equiv \|e_i\|_2$. Moreover, for vehicles in cyclic pursuit, $e_i = z_{i+1} - z_i$ and consequently $\sum_i^n e_i(t) \equiv 0$. Let $\xi := [\xi_1^\top, \xi_2^\top, \ldots, \xi_n^\top]^\top$. Then, by choosing a coordinate frame attached to (say) vehicle 1 and oriented with this vehicle's heading, this condition corresponds to constraints on the system described by the equations

$$g_1(\xi) = r_1 \sin\alpha_1 + r_2 \sin(\alpha_2 + \pi - \beta_1) + \cdots + r_n \sin(\alpha_n + (n-1)\pi - \beta_1 - \beta_2 - \cdots - \beta_{n-1}) = 0$$

$$g_2(\xi) = r_1 \cos\alpha_1 + r_2 \cos(\alpha_2 + \pi - \beta_1) + \cdots + r_n \cos(\alpha_n + (n-1)\pi - \beta_1 - \beta_2 - \cdots - \beta_{n-1}) = 0.$$

For vehicles numbered 1 and 2, Fig. 2 helps to illustrate how these constraint equations arise.

Also, due to cyclic pursuit

$$\sum_{i=1}^{n} \dot{\beta}_i(t) = 0 \Longrightarrow \sum_{i=1}^{n} \beta_i(t) \equiv c, \qquad \text{for all } t \geq 0$$

where the constant $c = -n\pi$ by our definition for β_i, which provides a final constraint

$$g_3(\xi) = \sum_{i=1}^{n} \beta_i + n\pi = 0 \bmod 2\pi.$$

These constraints are essential to our equilibrium and stability analyses, which follow in Sections V and VI, respectively.

C. Sample Simulation

Preliminary computer simulations suggest the possibility of achieving circular pursuit trajectories in the plane. Fig. 3 shows simulation results for a system of $n = 5$ vehicles, initially positioned at random, under the control law (7) with $k = 3$. Note that the vehicles converge to equally spaced motion around a circle of fixed radius with a pursuit graph that is similar to a regular pentagon.

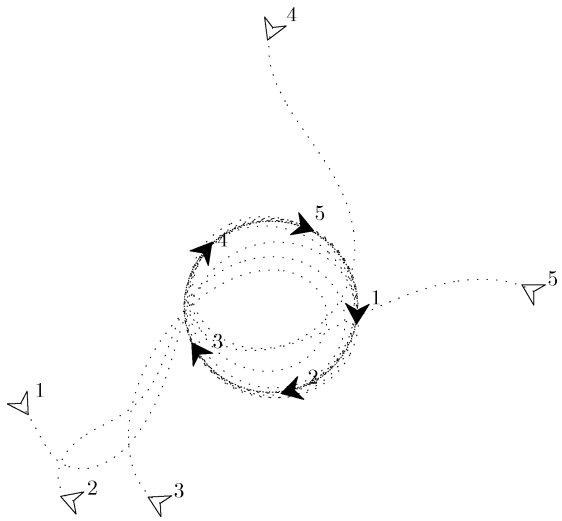

Fig. 3. Five vehicles subject to control law (7), with $k = 3$.

V. General Equilibria

In order to characterize the possible equilibrium formations for our multivehicle system (8), we need to adequately describe the state of our system's pursuit graph at equilibrium. The following definition for a regular polygon with coplanar vertices has been adapted from [28] to allow for vertices that are not necessarily distinct and for the directed edges of our pursuit graph.

Definition 2 (After [28, p. 93]): Let n and $d < n$ be positive integers so that $p := n/d > 1$ is a rational number. Let R be the positive rotation in the plane, about the origin, through angle $2\pi/p$ and let $z_1 \neq 0$ be a point in the plane. Then, the points $z_{i+1} = Rz_i$, $i = 1, 2, \ldots, n-1$ and edges $e_i = z_{i+1} - z_i$, $i = 1, 2, \ldots, n$, define a *generalized regular polygon*, which is denoted $\{p\}$.

By this definition, $\{p\}$ can be interpreted as a directed graph with vertices z_i (not necessarily distinct) connected by edges e_i as determined by the ordering of points. We say that $\{p\}$ is *positively oriented* if $d \leq n/2$ or *negatively oriented* if $d > n/2$.

Since p is rational, the period of R is finite and, when n and d are coprime, this definition is equivalent to the well-known definition of a regular polygon as a polygon that is both *equilateral* and *equiangular*. Moreover, when $d = 1$, $\{p = n\}$ is an *ordinary* regular polygon (i.e., its edges do not cross one another). However, when $d > 1$ is coprime to n, $\{p\}$ is a *star* polygon since its sides intersect at certain extraneous points, which are not included among the vertices [28, pp. 93–94]. If n and d have a common factor $m > 1$, then $\{p\}$ has $\tilde{n} = n/m$ distinct vertices and $\tilde{n}$ edges traversed m times. Note that the trivial case when $d = n$ has not been included since this corresponds to the geometrically uninteresting situation where the vertices are all coincident.

Fig. 4 illustrates some example possibilities for $\{p\}$ when $n = 9$. In the first instance, $\{9/1\}$ is an ordinary polygon. In the second instance, $\{9/2\}$ is a star polygon since 9 and 2 are

coprime. In the third instance, the edges of $\{9/3\}$ traverse a $\{3/1\}$ polygon three times, because $m = 3$ is a common factor of both 9 and 3.

Lemma 1 (After [28, p. 94]): The *internal angle* at every vertex of $\{p\}$ is given by $\psi = \pi\,(1 - 2d/n)$.

Note that the sign of ψ determines whether $\{p\}$ is positively or negatively oriented.

We are now ready to discuss the possible equilibrium formations for our system of n unicycles in cyclic pursuit.

Theorem 5: The $3n$-dimensional system (8) has $2(n-1)$ equilibrium points, described as follows: The r_i are all equal, $r_i = \bar{r}$; likewise, $\alpha_i = \bar{\alpha}$ and $\beta_i = \bar{\beta}$ for all $i \in \{1, 2, \ldots, n\}$. The $2(n-1)$ values of $\bar{r}$, $\bar{\alpha}$, and $\bar{\beta}$ are given by

$$\begin{aligned}\bar{\alpha} &= \pm\frac{\pi d}{n}, d = 1, 2, \ldots, n-1\\ \bar{\beta} &= \pi - 2\bar{\alpha}\\ \bar{r} &= \frac{2s}{k\bar{\alpha}}\sin\bar{\alpha}.\end{aligned}$$

Finally, at each equilibrium point, the related pursuit graph is a generalized regular polygon $\{n/d\}$, $d \in \{1, 2, \ldots, n-1\}$.

Proof: For $\dot{\beta}_i = 0$, (8c) yields $\alpha_i = \alpha_{i+1}$. Let $\bar{\alpha} \equiv \alpha_i$ at equilibrium. From the equilibrium condition $\dot{r}_i = 0$ of (8a), $\cos\bar{\alpha} = -\cos(\bar{\alpha} + \beta_i)$, which implies that either $\beta_i = \pi$ or $\beta_i = \pi - 2\bar{\alpha}$. However, at equilibrium (8b) yields $\bar{\alpha} = 0$ when $\beta_i = \pi$, implying that $\beta_i = \beta_{i+1}$ for all i. Let $\bar{\beta} \equiv \beta_i$ at equilibrium. Again, from the condition $\dot{\alpha}_i = 0$ of (8b)

$$r_i = \frac{s}{k\bar{\alpha}}\left[\sin\bar{\alpha} + \sin(\bar{\alpha} + \bar{\beta})\right], \qquad \text{for all } i \in \{1, 2, \ldots, n\}. \tag{9}$$

Therefore, $r_i = r_{i+1}$. Let $\bar{r} \equiv r_i$ at equilibrium.

For vehicles in cyclic pursuit, the system's pursuit graph $G = (V, E)$ has $\sum_{i=1}^{n} e(t) \equiv 0$. In particular, the constraint

$$\begin{aligned}g_2(\bar{\xi}) = \bar{r}[\cos\bar{\alpha} + \cos(\bar{\alpha} + \pi - \bar{\beta}) + \cdots\\ \cdots + \cos(\bar{\alpha} + (n-1)(\pi - \bar{\beta}))] = 0\end{aligned} \tag{10}$$

of Section IV-B must hold. However, when $\bar{\beta} = \pi$, (8b) implies that $\bar{\alpha} = 0$, which subsequently implies that the left-hand side of (10) equals $\bar{r}n \neq 0$. Thus, $\bar{\beta} = \pi$ (with $\bar{\alpha} = 0$) is not feasible for vehicles in cyclic pursuit.

Suppose $\bar{\alpha} > 0$. Since $r_i = r_{i+1}$, the system's pursuit graph G is equilateral (i.e., $\|e_i\|_2 = \|e_{i+1}\|_2$). Let ψ_i be the internal angle at each vertex of the pursuit graph. The pursuit graph is equiangular (i.e., $\psi_i = \psi_{i+1}$) since it can be checked using the geometry of Fig. 2 that the internal angle at each vertex is given by $\bar{\psi} \equiv \psi_i = \alpha_{i-1} + \beta_{i-1} - \alpha_i = \bar{\beta}$ at equilibrium. Therefore, by Definition 2, the pursuit graph must correspond to a generalized regular polygon $\{p\}$. By Lemma 1, the internal angle $\bar{\psi} = \bar{\beta}$ at each vertex of the polygon $\{p\}$ gives $\bar{\beta} = \pi\,(1 - 2d/n)$, which together with $\bar{\beta} = \pi - 2\bar{\alpha}$ implies that $\bar{\alpha} = \pi d/n$, where $d \in \{1, 2, \ldots, n-1\}$.

Repetition of the aforementioned argument for the case when $\bar{\alpha} < 0$ yields the remaining $n-1$ equilibrium points. By Definition 2, these $2(n-1)$ equilibrium points must satisfy the coordinate constraints of Section IV-B. ■

To clarify why there are $2(n-1)$ equilibria and only $n-1$ pursuit graphs, note that $\bar{\alpha} > 0$ and $\bar{\alpha} < 0$ correspond to counterclockwise and clockwise rotation of the system's pursuit graph at equilibrium, respectively. Also, notice that there are only $n-1$ distinct values of $\bar{r}$, since $\sin\bar{\alpha}/\bar{\alpha}$ is an even function.

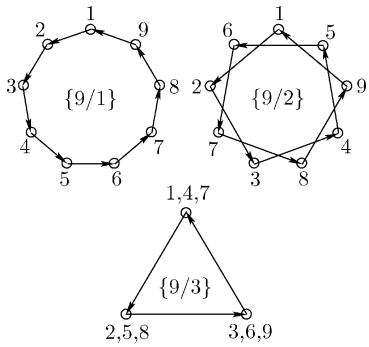

Fig. 4. Example generalized regular polygons $\{9/d\}$, $d \in \{1, 2, 3\}$.

The case when n and d of Theorem 5 are not coprime is physically undesirable (e.g., as in the polygon $\{9/3\}$ of Fig. 4) since it requires that multiple vehicles occupy the same point in space. From geometry, it is clear that, for each possible $\{n/d\}$ formation, the equilibrium angle $\bar{\alpha} = \pm\pi d/n$ corresponds exactly to a relative heading angle for each vehicle that points it in a direction that is *tangent* to the circle circumscribed by the vertices of the corresponding equilibrium polygon.

Corollary 2: At equilibrium, the vehicles traverse a circle of radius $\rho = sn/k\pi d$.

This can be shown by using Lemma 1, and the fact that, by elementary geometry [28, pp. 3, 94], $\bar{r} = 2\rho\cos(\bar{\psi}/2)$. By solving for ρ, we get the stated result.

Observe that the possible equilibrium formations depend only on our choice of gain k and forward speed s; in fact, only on the ratio $s : k$. Therefore, in what follows we assume $s = 1$ without loss of generality. Following Corollary 2, the radius about which the vehicles travel is determined by the designable parameter $k > 0$.

VI. Local Stability Analysis

In general, for a given number of vehicles $n \geq 2$, which $\{n/d\}$ equilibrium polygons are asymptotically stable, and for what values of k? In this section, we tackle the *local* stability question by linearizing about a general $\{n/d\}$ formation. Our solution then follows a procedure that is similar to the proof of Theorem 4 concerning linear agents, although the details are significantly more involved.

To facilitate notation, define $\tilde{\xi}_i := \xi_i - [\bar{r}, \bar{\alpha}, \bar{\beta}]^\top$ and let $q := p^{-1} = d/n$ so that $0 < q < 1$ and is rational. We write the kinematics of each vehicle subsystem (8) more compactly as $\dot{\xi}_i = f(\xi_i, \xi_{i+1})$. Linearizing each ξ_i model about an equilibrium point $[\bar{r}, \bar{\alpha}, \bar{\beta}]^\top$ gives n identical subsystems of the form $\dot{\tilde{\xi}}_i = A\tilde{\xi}_i + B\tilde{\xi}_{i+1}$ where

$$A = \begin{bmatrix} 0 & 2\sin(q\pi) & \sin(q\pi) \\ -\frac{1}{2}(kq\pi)^2\csc(q\pi) & -k & -\frac{1}{2}kq\pi\cot(q\pi) \\ 0 & k & 0 \end{bmatrix}$$

$$B = \begin{bmatrix} 0 & 0 & 0 \\ 0 & 0 & 0 \\ 0 & -k & 0 \end{bmatrix}.$$

If we view the *complete* multivehicle system as

$$\dot{\xi} = \hat{f}(\xi) \tag{11}$$

then its linearization about $\bar{\xi} \in \mathbb{R}^{3n}$ has the form $\dot{\tilde{\xi}} = \hat{A}\tilde{\xi}$ where $\hat{A} = \text{circ}[A, B, 0_{3\times 3}, \ldots, 0_{3\times 3}]$. In what follows, we aim to determine the stability properties of $\hat{A}$.

A. Coordinate Constraints

As in the linear agents problem, for every initial condition, (11) is constrained to evolve on a $\hat{f}$-invariant submanifold $\mathcal{M}$ of $\mathbb{R}^{3n}$. To see why this is the case, recall that under cyclic pursuit the system's pursuit graph at each instant satisfies $\sum_{i=1}^{n} e_i(t) \equiv 0$, resulting in the constraints of Section IV-B. These are essential with regards to understanding how the spectrum of $\hat{A}$ relates to the stability of a given $\{n/d\}$ equilibrium polygon.

Let $g(\xi) = [g_1(\xi), g_2(\xi), g_3(\xi)]^\top$. Then

$$\mathcal{M} = \left\{\xi \in \mathbb{R}^{3n} : g(\xi) = 0\right\} \subset \mathbb{R}^{3n} \tag{12}$$

defines a submanifold $\mathcal{M}$ of $\mathbb{R}^{3n}$.

Lemma 2: The submanifold $\mathcal{M}$ is invariant under $\hat{f}$.

See the Appendix for the proof.

Corollary 3: Since the submanifold $\mathcal{M}$ is invariant under $\hat{f}$, the tangent space $T_{\bar{\xi}}\mathcal{M}$ at every equilibrium point $\bar{\xi} \in \mathcal{M}$ is invariant under $\hat{A}$.

See the Appendix for the proof.

Therefore, by Corollary 3, there exists a change of basis for $\mathbb{R}^{3n}$ that transforms $\hat{A}$ into upper-triangular form

$$\begin{bmatrix} \hat{A}_{T_{\bar{\xi}}\mathcal{M}} & * \\ 0_{3\times(3n-3)} & \hat{A}^{\star}_{T_{\bar{\xi}}\mathcal{M}} \end{bmatrix}.$$

Lemma 3: In the quotient space $\mathbb{R}^{3n}/T_{\bar{\xi}}\mathcal{M}$, the induced linear transformation $\hat{A}^{\star}_{T_{\bar{\xi}}\mathcal{M}} : \mathbb{R}^{3n}/T_{\bar{\xi}}\mathcal{M} \to \mathbb{R}^{3n}/T_{\bar{\xi}}\mathcal{M}$ has (solely imaginary axis) eigenvalues

$$\lambda_1 = 0 \text{ and } \lambda_{2,3} = \pm jk\frac{\pi d}{n}.$$

Proof: Let $\varphi = \Phi(\xi)$ be the change of coordinates

$$\begin{aligned}\varphi_1 = r_1, \varphi_2 = \alpha_1, \ldots, \varphi_{3n-3} = \beta_{n-1}, \varphi_{3n-2} = g_1(\xi)\\ \varphi_{3n-1} = g_2(\xi), \varphi_{3n} = g_3(\xi).\end{aligned}$$

Partition these new coordinates into $\varphi = [\varphi_{\text{I}}^\top, \varphi_{\text{II}}^\top]^\top$ where $\varphi_{\text{I}} = [\varphi_1, \varphi_2, \ldots, \varphi_{3n-3}]^\top$ and $\varphi_{\text{II}} = [\varphi_{3n-2}, \varphi_{3n-1}, \varphi_{3n}]^\top$. Notice that the set of coordinates in φ_{II} are precisely the functions that define $\mathcal{M}$. Thus, in the new coordinates

$$\begin{aligned}\dot{\varphi}_{\text{I}} &= \left[\, I_{3n-3} \quad 0_{(3n-3)\times 3} \,\right] \hat{f}(\xi)\Big|_{\xi=\Phi^{-1}(\varphi)}\\ \dot{\varphi}_{\text{II}} &= \left[\frac{\partial g(\xi)}{\partial \xi}\hat{f}(\xi)\right]_{\xi=\Phi^{-1}(\varphi)}.\end{aligned}$$

Moreover, the equilibrium $\bar{\varphi} = \Phi(\bar{\xi})$ is equal to $\bar{\xi}$, except that the last three components are instead zero. By computing the linearization about this equilibrium, we get

$$\begin{aligned}\dot{\varphi}_{\text{I}} &= \left[\, I_{3n-3} \quad 0_{(3n-3)\times 3} \,\right] \hat{A}\varphi\\ \dot{\varphi}_{\text{II}} &= \left[\frac{\partial}{\partial \varphi}\left[\frac{\partial g(\xi)}{\partial \xi}\hat{f}(\xi)\right]_{\xi=\Phi^{-1}(\varphi)}\right]_{\bar{\varphi}} \varphi\\ &\overset{(*)}{=} \left[\frac{\partial}{\partial \varphi}\begin{bmatrix} -k\alpha_1 g_2(\xi) - \sin(g_3(\xi)) \\ k\alpha_1 g_1(\xi) + \cos(g_3(\xi)) - 1 \\ 0 \end{bmatrix}_{\xi=\Phi^{-1}(\varphi)}\right]_{\bar{\varphi}} \varphi\\ &= \left[\frac{\partial}{\partial \varphi}\begin{bmatrix} -k\varphi_2\varphi_{3n-1} - \sin\varphi_{3n} \\ k\varphi_2\varphi_{3n-2} + \cos\varphi_{3n} - 1 \\ 0 \end{bmatrix}\right]_{\bar{\varphi}} \varphi\\ &= \left[\begin{array}{ccc|ccc} 0 & \cdots & 0 & 0 & -k\bar{\alpha} & -1 \\ 0 & \cdots & 0 & k\bar{\alpha} & 0 & 0 \\ 0 & \cdots & 0 & 0 & 0 & 0 \end{array}\right] \varphi\\ &= \left[\, 0_{3\times(3n-3)} \quad \hat{A}^{\star}_{T_{\bar{\xi}}\mathcal{M}} \,\right] \varphi\end{aligned}$$

where the lengthy derivation of equivalence $(*)$ has been omitted for brevity. The 3×3 block $\hat{A}^{\star}_{T_{\bar{\xi}}\mathcal{M}}$ has eigenvalues $\lambda_{1,2,3} = \{0, \pm jk\bar{\alpha}\}$, with $\bar{\alpha} = \pm\pi d/n$ from Theorem 5. ■

Therefore, just as in the linear agents problem, when determining the stability of a given $\{n/d\}$ formation we can disregard these three imaginary axis eigenvalues of $\hat{A}$, and determine stability based on its remaining $3n-3$ eigenvalues.

B. Spectral Analysis of $\hat{A}$

Recall that $\hat{A}$ is a block circulant matrix of the form

$$\hat{A} = \text{circ}[A, B, 0_{3\times 3}, \ldots, 0_{3\times 3}].$$

In what follows, we exploit this fact and our knowledge of block circulant matrices from Section II-C to further isolate the eigenvalues of $\hat{A}$.

Lemma 4: The eigenvalues of $\hat{A}$ are the collection of all eigenvalues of

$$\begin{aligned} &A + B\\ &A + \omega B\\ &A + \omega^2 B\\ &\vdots\\ &A + \omega^{n-1} B\end{aligned}$$

where $\omega^{i-1} := e^{2(i-1)\pi j/n} \in \mathbb{C}$ is the ith of n roots of unity.

Proof: By Theorem 3, since $\hat{A}$ is block circulant it can be diagonalized using the Fourier matrix F_n; specifically

$$\text{diag}(D_1, D_2, \ldots, D_n) = (F_n \otimes I_3)\hat{A}(F_n \otimes I_3)^*$$

where the n 3×3 diagonal blocks D_i are given by

$$\begin{bmatrix} D_1 \\ D_2 \\ \vdots \\ D_n \end{bmatrix} = \left(\sqrt{n}F_n^* \otimes I_3\right)\begin{bmatrix} M_1 \\ M_2 \\ \vdots \\ M_n \end{bmatrix}$$

with $M_1 = A$, $M_2 = B$, and $M_i = 0_{3\times 3}$ for $i = \{3, 4, \ldots, n\}$. Expanding this for each block D_i, we get

$$\begin{aligned} D_1 &= A + B \\ D_2 &= A + \omega B \\ D_3 &= A + \omega^2 B \\ &\vdots \\ D_n &= A + \omega^{n-1} B \end{aligned}$$

as the diagonal blocks for diagonalized $\hat{A}$. This implies that the eigenvalues of $\hat{A}$ must be the collection of all eigenvalues of $A + \omega^{i-1}B$, $i = 1, 2, \ldots, n$. ∎

Therefore, each diagonal block has the same form $D_i = A + \omega^{i-1}B$, $i \in \{1, 2, \ldots, n\}$, given by

$$D_i = \begin{bmatrix} 0 & 2\sin(q\pi) & \sin(q\pi) \\ -\frac{1}{2}(kq\pi)^2 \csc(q\pi) & -k & -\frac{1}{2}kq\pi\cot(q\pi) \\ 0 & k(1-\omega^{i-1}) & 0 \end{bmatrix}.$$

From Lemma 4, we observe two facts. The first is that the eigenvalues of $D_1 = A + B$ are among the eigenvalues of $\hat{A}$ for every n. The characteristic polynomial of D_1 is

$$p_{D_1}(\lambda) = \lambda^3 + k\lambda^2 + (kq\pi)^2\lambda = \lambda\left(\lambda^2 + k\lambda + (kq\pi)^2\right)$$

so the eigenvalues of D_1 are

$$\begin{aligned} \lambda_1 &= 0 \\ \lambda_{2,3} &= -\frac{k}{2} \pm j\frac{k}{2}\sqrt{4(q\pi)^2 - 1}. \end{aligned} \tag{13}$$

As predicted by Lemma 3, we have discovered one zero eigenvalue, while the remaining eigenvalues have $\mathrm{Re}(\lambda_{2,3}) < 0$ for every $0 < q < 1$ and $k > 0$.

The second fact is that, when the number of vehicles n is even, the eigenvalues of the matrix $D_{i^*} = A - B$, with $i^* := (n/2) + 1$, are among the eigenvalues of $\hat{A}$. The characteristic polynomial of D_{i^*} is

$$p_{D_{i^*}}(\lambda) = \lambda^3 + k\lambda^2 + k^2\left[(q\pi)^2 + q\pi\cot(q\pi)\right]\lambda + k^3(q\pi)^2$$

for which we can construct the Routh array

$$\begin{array}{c|cc} \lambda^3 & 1 & k^2[(q\pi)^2 + q\pi\cot(q\pi)] \\ \lambda^2 & k & k^3(q\pi)^2 \\ \lambda^1 & k^2 q\pi\cot(q\pi) & 0 \\ \lambda^0 & k^3(q\pi)^2 & 0 \end{array}. \tag{14}$$

By the Routh–Hurwitz criterion, for stability we would need that $\cot(q\pi) > 0$ (due to the λ^1 element of the first column) or, equivalently, $0 < q < 1/2$. Moreover, in the special case when $q = 1/2$ the characteristic polynomial factors as

$$p_{D_{i^*}}(\lambda) = \left(\lambda + j\frac{k\pi}{2}\right)\left(\lambda - j\frac{k\pi}{2}\right)(\lambda + k) \tag{15}$$

which yields two imaginary axis eigenvalues, as predicted by Lemma 3, and one stable eigenvalue. Let us consider the simplest case, when $n = 2$.

Proposition 1: The $\{2/1\}$ equilibrium polygon is locally asymptotically stable.

Proof: When $n = 2$ the matrix $\hat{A}$ has the form

$$\hat{A} = \begin{bmatrix} A & B \\ B & A \end{bmatrix}.$$

By Lemma 4, the eigenvalues (13) of $D_1 = A + B$ must be among those of $\hat{A}$. Moreover, $i^* = 2$ and so the eigenvalues of $D_2 = A - B$, which are the roots of (15), must be the remaining eigenvalues of $\hat{A}$. We disregard the imaginary axis eigenvalues according to Lemma 3 and conclude that the $\{2/1\}$ polygon is locally asymptotically stable. ∎

We now continue investigating the general case $n \geq 2$.

Lemma 5: The stability of $\hat{A}$ is independent of $k > 0$.

Proof: Suppose we have block diagonalized $\hat{A}$ into n diagonal blocks $D_i = A + \omega^{i-1}B$ according to Lemma 4. The claim of Lemma 5 is then obvious when each block D_i is factored as $D_i = kT\tilde{D}_iT^{-1}$, where $T = \mathrm{diag}[(1/k)\sin(q\pi), 1, 1]$ (recall $0 < q < 1$) and

$$\tilde{D}_i = \begin{bmatrix} 0 & 2 & 1 \\ -\frac{1}{2}(q\pi)^2 & -1 & -\frac{1}{2}q\pi\cot(q\pi) \\ 0 & 1-\omega^{i-1} & 0 \end{bmatrix}$$

so that $\sigma(D_i) = k\sigma(\tilde{D}_i)$, where $\sigma(\cdot)$ denotes the spectrum of a matrix. Since $k > 0$, the stability of the matrix $\tilde{D}_i$ implies the stability of D_i. ∎

Therefore, whether a specific $\{n/d\}$ polygon is stable or not is independent of the chosen gain $k > 0$, and we can proceed by studying the transformed blocks $\tilde{D}_i$. In other words, for a given n, only the density d influences the stability of $\hat{A}$.

C. Stable Equilibrium Polygons

Let us briefly recapitulate. About a given $\{n/d\}$ equilibrium polygon, our linearized multivehicle system has the form $\dot{\xi} = \hat{A}\xi$, where $\hat{A}$ is a block circulant matrix. We have seen (through Lemma 3) that $\hat{A}$ has exactly three imaginary axis eigenvalues that do not influence the stability of a given $\{n/d\}$ formation. Capitalizing on the block circulant structure of $\hat{A}$, we block diagonalized $\hat{A}$ into n 3×3 blocks, D_i. We then showed (through Lemma 5) that the stability of each matrix D_i, and hence the stability of $\hat{A}$, is independent of $k > 0$, leaving that stability is dependent only on d for a given n via the 3×3 transformed matrices $\tilde{D}_i$.

Unfortunately, the blocks $\tilde{D}_i$ are, in general, *complex* matrices. To be explicit about this fact, we can write the n roots of unity $\omega^{i-1} = w_i + jz_i \in \mathbb{C}$, where

$$w_i = \cos\left(2\pi\frac{i-1}{n}\right) \text{ and } z_i = \sin\left(2\pi\frac{i-1}{n}\right).$$

In this general case, the characteristic polynomial of $\tilde{D}_i$ is

$$p_{\tilde{D}_i}(\lambda) = \lambda^3 + \lambda^2 + (a_2 + jb_2)\lambda + (a_3 + jb_3) \tag{16}$$

with coefficients

$$\begin{aligned} a_2 &= (q\pi)^2 + \frac{1}{2}q\pi(1 - w_i)\cot(q\pi) \\ b_2 &= -\frac{1}{2}q\pi z_i\cot(q\pi) \\ a_3 &= \frac{1}{2}(1 - w_i)(q\pi)^2 \\ b_3 &= -\frac{1}{2}z_i(q\pi)^2. \end{aligned} \tag{17}$$

Theorem 6 (After [29, Th. 3.16, p. 180]): Consider a complex polynomial of the third degree

$$p(\lambda) = \lambda^3 + c_1\lambda^2 + c_2\lambda + c_3$$

where $c_1, c_2, c_3 \in \mathbb{C}$. Define the Hermitian matrix

$$H = \begin{bmatrix} c_1 + \bar{c}_1 & c_2 - \bar{c}_2 & c_3 + \bar{c}_3 \\ -c_2 + \bar{c}_2 & \bar{c}_2 + c_2 - \bar{c}_3 - c_3 & c_3 - \bar{c}_3 \\ c_3 + \bar{c}_3 & -c_3 + \bar{c}_3 & c_2\bar{c}_3 + \bar{c}_2 c_3 \end{bmatrix}.$$

The polynomial $p(\lambda)$ is asymptotically stable if and only if H is positive definite.

Here, $\bar{c}$ denotes the complex conjugate of c. Also, this theorem is equivalent to a variation of the Routh–Hurwitz criterion for complex polynomials [29, p. 179]. Recall that a Hermitian matrix H is positive definite if and only if its leading principal minors, which we denote h_1, h_2, and h_3, are positive. Suppose we apply Theorem 6 to the characteristic polynomial (16) of $\tilde{D}_i$. Computing the leading principal minors of the corresponding H gives

$$\begin{aligned} h_1 &= 2 \\ h_2 &= 4(a_2 - a_3 - b_2^2) \\ h_3 &= 8(a_2^2 a_3 + a_2 b_2 b_3 - 2a_2 a_3^2 - 3a_3 b_2 b_3 \\ &\quad - b_3^2 - a_3 b_2^2 a_2 - b_2^3 b_3 + a_3^3). \end{aligned}$$

Clearly, $h_1 > 0$. Stability of a given $\tilde{D}_i$ matrix is therefore dependent on the signs of h_2 and h_3. For stability, substituting (17) and using $z_i^2 = 1 - w_i^2$, we would need that

$$h_2(q, w_i) = 2(1 + w_i)q\pi + 2(1 - w_i)\cot(q\pi) - (1 - w_i^2)q\pi\cot^2(q\pi) > 0 \quad (18)$$

for the second leading principal minor, and

$$\begin{aligned} h_3(q, w_i) = {} & (1 + w_i - w_i^2 - w_i^3)[(q\pi)^2 + q\pi\cot(q\pi)] \\ & -(1 - w_i - w_i^2 + w_i^3)[(q\pi)^2\cot^2(q\pi) + q\pi\cot^3(q\pi)] \\ & +2(1 - 2w_i + w_i^2)\cot^2(q\pi) - 2(1 - w_i^2) > 0 \end{aligned} \quad (19)$$

for the third leading principal minor. The decision to write h_2 and h_3 as functions of the real component w_i rather than the imaginary component z_i was arbitrary. In what follows, we will use these functions h_2 and h_3 to determine which $\{n/d\}$ equilibrium polygons are stable and which are not.

For a given n, define the set of w_i by

$$\mathcal{W}_n = \left\{ w_i = \mathrm{Re}(\omega^{i-1}) : \; i = 1, 2, \ldots, n \right\}.$$

Lemma 6: Every $\{n/d\}$ equilibrium polygon with $n/2 < d < n$ is unstable.

Proof: When n is even, we have already seen that the eigenvalues of $A - B$ (a *real* matrix) are among the eigenvalues of $\hat{A}$ (i.e., if $i^* := (n/2) + 1$, $w_{i^*} = -1$ is always a root of unity). By the Routh array (14), $D_{i^*} = A - B$ is unstable when $1/2 < (d/n) < 1$, or equivalently $(n/2) < d < n$.

When n is odd, look at h_2 and consider the set of points that are *not* stable

$$\mathcal{H}_2 = \{(\mu, w) : h_2(\mu, w) \le 0, \mu \in (0, 1), w \in (-1, 1)\}$$

which is illustrated by region U of Fig. 5(a). Note that we are taking μ and w on a continuum, whereas the arguments of h_2 in (18), q and $w_i \in \mathcal{W}_n$, take on rational and discrete values, respectively.

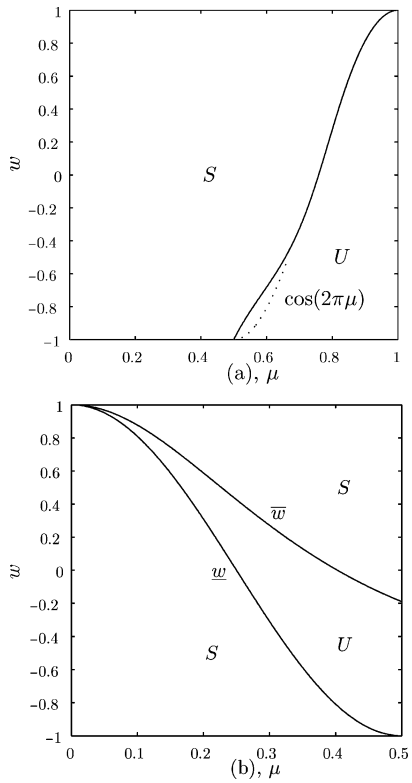

Fig. 5. Parameter w as a function of μ for the leading principal minors (a) h_2 and (b) h_3 of H. In (a), U denotes the closed set of points where $h_2 \le 0$. In (b), U denotes the closed set of points where $h_3 \le 0$.

Let $\mathrm{int}\mathcal{H}_2$ denote the interior of $\mathcal{H}_2$. It is a fact that the pair $(\mu, \cos(2\pi\mu)) \in \mathrm{int}\mathcal{H}_2$ for every $\mu \in (1/2, 2/3]$, as illustrated by the dotted line in Fig. 5(a). This fact, which is most easily checked numerically, will be useful in what follows.

Let $d^* := (n+1)/2$, the smallest integer satisfying the condition $n/2 < d < n$ of the lemma. Let $i^* := d^* + 1$, which gives

$$w_{i^*} = \mathrm{Re}(\omega^{d^*}) = \cos\left(\frac{2\pi d^*}{n}\right) \in \mathcal{W}_n.$$

Note that $1/2 < d^*/n \le 2/3$ for every $n \ge 3$, which (by the previously stated fact) implies that for every $n \ge 3$ there exists a $w_{i^*} \in \mathcal{W}_n$ such that $(d^*/n, w_{i^*}) \in \mathrm{int}\mathcal{H}_2$, i.e., every $\{n/d^*\}$ polygon is unstable.

It is left to show that the remaining densities $d^* < d < n$ satisfying the condition $n/2 < d < n$ of the lemma are also unstable. Since $d^*/n < d/n < 1$, the point $(d/n, w_{i^*}) \in \mathrm{int}\mathcal{H}_2$ also lives in the region U. This is because it lies directly to the right of the unstable point $(d^*/n, w_{i^*}) \in \mathrm{int}\mathcal{H}_2$ in Fig. 5(a), which concludes the proof. ■

Before stating our main result, consider the set of points that are *not* stable

$$\mathcal{H}_3 = \{(\mu, w) : h_3(\mu, w) \le 0, \mu \in \left(0, \frac{1}{2}\right], w \in (-1, 1)\} \quad (20)$$

which is illustrated by the region U of Fig. 5(b). Define the following functions:

$$\overline{w}(\mu) := \frac{2\tan(\mu\pi)}{\mu\pi[1+\mu\pi\tan(\mu\pi)]} - 1$$
$$\underline{w}(\mu) := \cos(2\pi\mu)$$

which describe the upper and lower boundaries of the region U in Fig. 5(b). These functions were obtained by solving[3] the equation $h_3(\mu, w) = 0$ on the relevant domain $\mu = (0, 1/2]$ and $w \in (-1, 1)$ and numerically checking that the region U indeed corresponds to the set $\mathcal{H}_3$. As a result, the definition (20) is equivalent to

$$\mathcal{H}_3 = \{(\mu, w) : \mu \in \left(0, \frac{1}{2}\right], w \in [\underline{w}(\mu), \overline{w}(\mu)]\}.$$

Theorem 7 (Main Stability Result): A given $\{n/d\}$ equilibrium polygon is locally asymptotically stable if and only if $0 < d \leq n/2$ and

$$\underline{w}\left(\frac{d-1}{n}\right) > \overline{w}\left(\frac{d}{n}\right). \tag{21}$$

Proof: According to the proof of Lemma 6, $h_2 < 0$ for every $\{n/d\}$ polygon with $n/2 < d < n$. Thus, a necessary condition for stability is that $0 < d \leq n/2$. Notice that $h_2 > 0$ for every $0 < d < n/2$ [see Fig. 5(a)]. Let's proceed by assuming that this condition holds for the given $\{n/d\}$ polygon. We will consider the special case when $d = n/2$ separately. Moreover, observe that every matrix D_i has a complex conjugate matrix D_{n-i+2}, hence the spectrum of D_i and that of its conjugate are also complex conjugates.

Define $i^* := d + 1$ so that $w_{i^*} = \cos(2\pi(d/n)) \equiv \underline{w}(d/n)$. Thus, the point $(d/n, w_{i^*})$ lies exactly on the lower boundary of $\mathcal{H}_3$ in Fig. 5(b). Together, the matrix D_{i^*} and its conjugate D_{n-i^*+2} have two imaginary axis eigenvalues (one each) of the form $\lambda = \pm jk\pi(d/n)$, while the remaining eigenvalues have $\mathrm{Re}(\lambda) \neq 0$. These facts were verified with the assistance of computer algebra software. The eigenvalues with $\mathrm{Re}(\lambda) \neq 0$ cannot be unstable, otherwise the point $(d/n, w_{i^*})$ would not lie on the boundary of $\mathcal{H}_3$. According to Lemma 3, we can disregard the two imaginary axis eigenvalues, and also the zero eigenvalue of D_1, since they have no connection to the stability of the given $\{n/d\}$ polygon. Since the point $(d/n, w_{i^*})$ lies on the lower boundary of $\mathcal{H}_3$, all points $(d/n, w_i)$, $w_i \in \mathcal{W}_n$ with $w_i < w_{i^*}$ lie outside the unstable set $\mathcal{H}_3$. Thus, we turn our attention to the points $(d/n, w_i)$, $w_i \in \mathcal{W}_n$ with $w_i > w_{i^*}$.

Define the index $i' := i^* - 1 = d$, corresponding to $w_{i'} \in \mathcal{W}_n$, $w_{i'} > w_{i^*}$ that is *closest* to w_{i^*}. This new value is given by $w_{i'} = \cos(2\pi((d-1)/n)) \equiv \underline{w}((d-1)/n)$. If $w_{i'} > \overline{w}(d/n)$, then the point $(d/n, w_i) \notin \mathcal{H}_3$ for all $w_i \in \mathcal{W}_n$, $w_i > w_{i^*}$. Therefore, by Theorem 6, stability is equivalent to $\underline{w}((d-1)/n) > \overline{w}(d/n)$.

In the special case when $d = n/2$, the matrix D_{i^*} is *real* and has eigenvalues according to the roots of (15). Therefore, one is stable and the remaining two imaginary axis eigenvalues should be ignored according to Lemma 3. The rest of the proof follows as for $0 < d < n/2$. ∎

[3]This solution was obtained with the aid of computer algebra software.

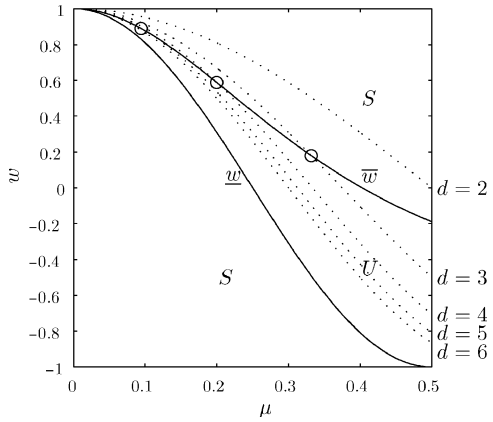

Fig. 6. Function $\underline{w}(\mu - (\mu/d))$ shown for $d \in \{2, 3, 4, 5, 6\}$ (dotted), superimposed on Fig. 5(b). Circles indicate intersection with $\overline{w}(\mu)$.

In the following sequence of corollaries, we employ this main result to explicitly disclose which $\{n/d\}$ equilibrium polygons are stable and which are not.

Corollary 4: Every $\{n/1\}$ polygon is locally asymptotically stable.

Proof: Let $d = 1$ and $n \geq 2$. Then, $\underline{w}(0) = 1$ and $\overline{w}(d/n) < 1$ for every $n \in \{2, 3, \ldots\}$, from Fig. 5(b), so that the conditions of Theorem 7 are satisfied. ∎

Recall that the variable μ is intended to represent d/n. Thus, with reference to Fig. 5(b), for some *fixed* density d the condition for stability (21) is equivalent to

$$\underline{w}\left(\mu - \frac{\mu}{d}\right) > \overline{w}(\mu). \tag{22}$$

The graphs of $\underline{w}(\mu - (\mu/d))$ versus μ for $d \in \{2, 3, 4, 5, 6\}$ are illustrated by the dotted curves of Fig. 6. Notice that only when $d \in \{3, 4, 5\}$ does $\underline{w}(\mu - (\mu/d))$ intersect the curve $\overline{w}(\mu)$ on the real interval $\mu \in (0, 1/2]$.

Corollary 5: Every $\{n/2\}$ polygon with $n \geq 4$ is locally asymptotically stable.

Proof: When $d = 2$, the necessary condition $0 < d \leq n/2$ of Theorem 7 dictates that $n \geq 4$. Moreover, from Fig. 6, inequality (21) is satisfied for every $n \in \{4, 5, \ldots\}$. ∎

Corollary 6: Every $\{n/d\}$ polygon with $d \geq 6$ is unstable.

Proof: When $d \geq 6$, from Fig. 6, (21) is never satisfied; i.e., $\underline{w}((d-1)/n) < \overline{w}(d/n)$ for every $6 \leq d \leq n/2$. ∎

Using Theorem 7 and Fig. 6, we can now determine the stability of the remaining polygons $\{n/d\}$, $d \in \{3, 4, 5\}$ by replacing (22) with an equality.

Corollary 7: For a $\{n/d\}$ polygon with $d \in \{3, 4, 5\}$, let $\bar{\mu}$ be the unique solution to $\underline{w}(\mu - (\mu/d)) = \overline{w}(\mu)$. Then, $\{n/d\}$ is locally asymptotically stable if and only if $d < \bar{\mu}n$.

Proof: For $d \in \{3, 4, 5\}$ the graphs of $\underline{w}(\mu - (\mu/d))$ and $\overline{w}(\mu)$ intersect exactly once in the domain $\mu \in (0, 1/2]$ (see Fig. 6). Let $\bar{\mu}$ be this point of intersection and note that $d/n < \bar{\mu}$ results in stability, while $d/n > \bar{\mu}$ gives instability, per Theorem 7. ∎

These points of intersection $\bar{\mu}$ (computed numerically) are given by the $(d, \bar{\mu})$ pairs (3, 0.331 868), (4, 0.199 945), and (5, 0.094 211), and shown as circles in Fig. 6. Employing these values, we find that polygon {10/3} is stable, while {9/3} is not. Similarly, {21/4} is stable, while {20/4} is not, and finally

TABLE I
EQUILIBRIUM POLYGONS WITH STABLE POLYGONS SHADED

$d=1$	2	3	4	5	6
{2/1}	{3/2}	{4/3}	{5/4}	{6/5}	{7/6}
{3/1}	{4/2}	{5/3}	{6/4}	{7/5}	{8/6}
⋮	⋮	⋮	⋮	⋮	⋮
{7/1}	{8/2}	{9/3}	{10/4}	{11/5}	{12/6}
{8/1}	{9/2}	{10/3}	{11/4}	{12/5}	{13/6}
⋮	⋮	⋮	⋮	⋮	⋮
{17/1}	{18/2}	{19/3}	{20/4}	{21/5}	{22/6}
{18/1}	{19/2}	{20/3}	{21/4}	{22/5}	{23/6}
⋮	⋮	⋮	⋮	⋮	⋮
{49/1}	{50/2}	{51/3}	{52/4}	{53/5}	{54/6}
{50/1}	{51/2}	{52/3}	{53/4}	{54/5}	{55/6}
⋮	⋮	⋮	⋮	⋮	⋮

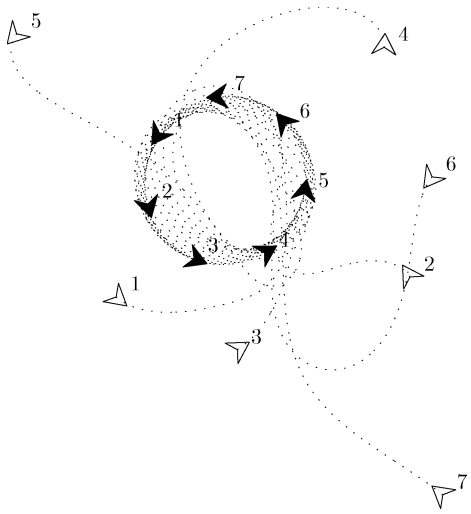

Fig. 7. Fixed forward speed pursuit generating a $\{7/1\}$ formation.

{54/5} is stable, while {53/5} is not. Table I lists all possible equilibrium polygons and gives their stability.

D. Sample Simulations

Figs. 7 and 8 show computer simulation results for $n = 7$ vehicles, where in each case the forward speed $s = 1$ and gain $k = 4$. However, due to differing initial conditions, the vehicles of Fig. 7 form a $\{7/1\}$ polygon, whereas the vehicles of Fig. 8 converge to a $\{7/2\}$ equilibrium formation.

VII. CONCLUSION

Over the last century, several pursuit problems have appeared in the mathematical literature. In this paper, our motivation has been to follow historical development and at the same time advance these ideas for potential engineering use by proposing a cyclic pursuit strategy for multivehicle systems that is in essence a nonlinear (unicycle) version of the so-called "bugs" problem from mathematics. The current research is further motivated by the prevalence of similar distributed control algorithms found in nature [4], [30]. Moreover, the notion of local interaction laws for formation control is, from an engineering standpoint, clearly very appealing.

To summarize, we have studied one particularly intuitive control law that achieves circular pursuit patterns in the plane. It

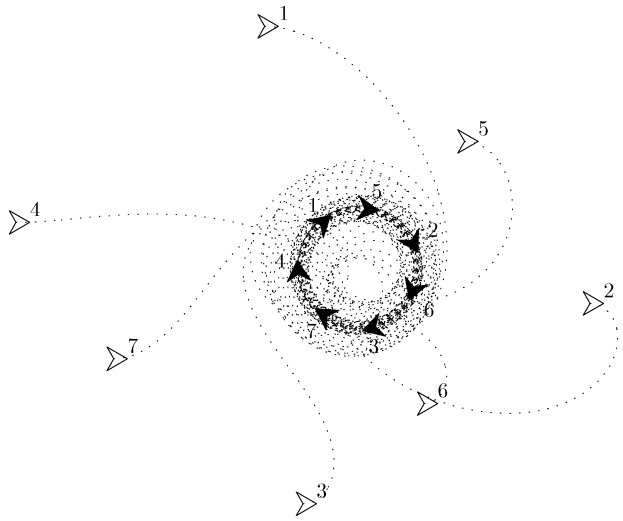

Fig. 8. Fixed forward speed pursuit generating a $\{7/2\}$ formation.

was shown that, under this control law, the multivehicle system's equilibrium formations are generalized regular polygons and that the system's global behavior can be changed through appropriate controller gain assignments. This type of formation strategy might have, for example, potential application in the deployment of distributed sensor arrays, enabling scientists to collect simultaneous seismological, meteorological, or other pertinent environmental data on planetary exploration missions [31]. A local stability analysis, which exploited the system's inherent circulant structure, revealed exactly which equilibrium formations are asymptotically stable, the result of which is surprisingly nonintuitive. Of course, the current study has assumed identical kinematic unicycles, ideal sensing conditions, and has not considered the problem of collisions, issues that would have to be dealt with prior to implementation as useful distributed control strategy. In conclusion, it is hoped that this work might serve as a basis for continuing research on the subject of pursuit and its applicability to the distributed control of multiagent systems.

APPENDIX
PROOF OF LEMMA 2 AND COROLLARY 3

The proof of Lemma 2 follows as a consequence of the lemma given here.

Lemma 7: The submanifold $\mathcal{M}$ of $\mathbb{R}^{3n}$ is invariant under $\hat{f}$ if and only if

$$\frac{\partial g(\xi)}{\partial \xi}\hat{f}(\xi) = 0, \qquad \text{for every } \xi \in \mathcal{M}. \tag{23}$$

Proof: At every point $\xi \in \mathcal{M}$ we can define a three-dimensional plane that is orthogonal to the $(3n-3)$-dimensional tangent plane $T_\xi\mathcal{M}$ by [32, App. A.5]

$$(T_\xi\mathcal{M})^\perp = \operatorname{span}\{dg_1(\xi), dg_2(\xi), dg_3(\xi)\}.$$

Therefore, the inner product

$$\left\langle dg_i^\top(\xi), \hat{f}(\xi)\right\rangle = 0, \qquad \text{for every } i \in \{1,2,3\}, \xi \in \mathcal{M}$$

is equivalent to

$$\hat{f}(\xi) \in T_\xi\mathcal{M}, \qquad \text{for every } \xi \in \mathcal{M}.$$

Hence, $\hat{f}$ is tangent to $\mathcal{M}$ everywhere on $\mathcal{M} \iff \mathcal{M}$ is invariant under $\hat{f}$. ■

Equivalence $(*)$ from the proof of Lemma 3 provides the necessary and sufficient condition (23) of Lemma 7, from which Lemma 2 directly follows.

Differentiating (23) gives

$$\hat{f}^\top(\xi)\frac{\partial}{\partial \xi}\left(\frac{\partial g_i^\top(\xi)}{\partial \xi}\right)+\frac{\partial g_i(\xi)}{\partial \xi}\frac{\partial \hat{f}(\xi)}{\partial \xi}=0, \qquad \text{for } i=1,2,3.$$

At every equilibrium point $\bar{\xi} \in \mathcal{M}$, $\hat{f}(\bar{\xi})=0$, which implies

$$\left[\frac{\partial g(\xi)}{\partial \xi}\right]_{\bar{\xi}} \hat{A}=0.$$

In other words, at $\bar{\xi} \in \mathcal{M}$, the columns of $\hat{A}$ must lie in the tangent space $T_{\bar{\xi}}\mathcal{M}$, so $T_{\bar{\xi}}\mathcal{M}$ must be an $\hat{A}$-invariant subspace of $\mathbb{R}^{3n}$, which proves Corollary 3.

REFERENCES

[1] T. D. Barfoot, E. J. P. Earon, and G. M. T. D'Eleuterio, "Controlling the masses: Control concepts for multi-agent mobile robotics," presented at the 2nd Canadian Space Exploration Workshop, Calgary, AB, Canada, Oct. 1999.

[2] C. Canudas-de-Wit and A. D. NDoudi-Likoho, "Nonlinear control for a convoy-like vehicle," *Automatica*, vol. 36, pp. 457–462, 2000.

[3] A. R. Girard, J. B. de Sousa, and J. K. Hedrick, "An overview of emerging results in networked multi-vehicle systems," in *Proc. 40th IEEE Conf. Decision and Control*, Orlando, FL, Dec. 2001, pp. 1485–1490.

[4] C. W. Reynolds, "Flocks, herds, and schools: A distributed behavioral model," *Comput. Graph.*, vol. 21, no. 4, pp. 25–34, July 1987.

[5] T. Balch and R. C. Arkin, "Behavior-based formation control for multirobot teams," *IEEE Trans. Robot. Automat.*, vol. 14, pp. 926–939, Dec. 1998.

[6] Y. U. Cao, A. S. Fukunaga, and A. B. Kahng, "Cooperative mobile robotics: Antecedents and directions," *Auton. Robot.*, vol. 4, pp. 1–23, 1997.

[7] M. J. Matarić, "Issues and approaches in the design of collective autonomous agents," *Robot. Auton. Syst.*, vol. 16, pp. 321–331, 1995.

[8] K. Sugihara and I. Suzuki, "Distributed motion coordination of multiple mobile robots," in *Proc. 5th IEEE Int. Symp. Intelligent Control*, 1990, pp. 138–143.

[9] V. Braitenberg, *Vehicles: Experiments in Synthetic Psychology*. Cambridge, MA: MIT Press, 1984.

[10] P. K. C. Wang, "Navigation strategies for multiple autonomous mobile robots moving in formation," in *Proc. IEEE/RSJ Int. Workshop Intelligent Robots and Systems*, Tsukuba, Japan, Sept. 1989, pp. 486–493.

[11] I. Suzuki and M. Yamashita, "Distributed anonymous mobile robots: Formation of geometric patterns," *SIAM J. Computing*, vol. 28, no. 4, pp. 1347–1363, 1999.

[12] E. W. Justh and P. S. Krishnaprasad, "A simple control law for UAV formation flying," Inst. Syst. Res., Univ. Maryland, College Park, MD, Tech. Rep. TR 2002–38, 2002.

[13] ——, "Steering laws and continuum models for planar formations," in *Proc. 42nd IEEE Conf. Decision and Control*, Maui, HI, Dec. 2003, pp. 3609–3614.

[14] A. Jadbabaie, J. Lin, and A. S. Morse, "Coordination of groups of mobile autonomous agents using nearest neighbor rules," *IEEE Trans. Automat. Contr.*, vol. 48, pp. 988–1001, June 2003.

[15] A. M. Bruckstein, "Why the ant trails look so straight and nice," *Math. Intell.*, vol. 15, no. 2, pp. 59–62, 1993.

[16] V. Gazi, "Stability analysis of swarms," Ph.D. dissertation, The Ohio State Univ., Columbus, OH, 2002.

[17] V. Gazi and K. M. Passino, "Stability analysis of swarms," in *Proc. Amer. Control Conf.*, Anchorage, AK, May 2002, pp. 1813–1818.

[18] A. Bernhart, "Polygons of pursuit," *Scripta Mathematica*, vol. 24, pp. 23–50, 1959.

[19] A. Watton and D. W. Kydon, "Analytical aspects of the n-bug problem," *Amer. J. Phys.*, vol. 37, pp. 220–221, 1969.

[20] M. S. Klamkin and D. J. Newman, "Cyclic pursuit or 'The three bugs problem'," *Amer. Math. Month.*, vol. 78, no. 6, pp. 631–639, June/July 1971.

[21] F. Behroozi and R. Gagnon, "Cylcic pursuit in a plane," *J. Math. Phys.*, vol. 20, no. 11, pp. 2212–2216, 1979.

[22] T. J. Richardson, "Non-mutual captures in cyclic pursuit," *Ann. Math. Artif. Intell.*, vol. 31, pp. 127–146, 2001.

[23] A. M. Bruckstein, N. Cohen, and A. Efrat, "Ants, crickets and frogs in cyclic pursuit," Center Intell. Syst., Technion-Israel Inst. Technol., Haifa, Israel, Tech. Rep. 9105, 1991.

[24] J. A. Marshall, M. E. Broucke, and B. A. Francis, "A pursuit strategy for wheeled-vehicle formations," in *Proc. 42nd IEEE Conf. Decision and Control*, Maui, HI, Dec. 2003, pp. 2555–2560.

[25] J. P. Desai, J. Ostrowski, and V. Kumar, "Controlling formations of multiple mobile robots," in *Proc. 1998 IEEE Int. Conf. Robotics and Automation*, Leuven, Belgium, May 1998, pp. 2864–2869.

[26] P. J. Davis, *Circulant Matrices*, 2nd ed. New York: Chelsea, 1994.

[27] Z. Lin, M. E. Broucke, and B. A. Francis, "Local control strategies for groups of mobile autonomous agents," in *Proc. 42nd IEEE Conf. Decision and Control*, Maui, HI, Dec. 2003, pp. 1006–1011.

[28] H. S. M. Coxeter, *Regular Polytopes*. London, U.K.: Methuen & Co. Ltd, 1948.

[29] S. Barnett, *Polynomials and Linear Control Systems*. New York: Marcel Dekker, 1983, Monographs and Textbooks in Pure and Applied Mathematics Series.

[30] J. K. Parrish, S. V. Viscido, and D. Grünbaum, "Self-organized fish schools: An examination of emergent properties," *Biol. Bull.*, vol. 202, pp. 296–305, June 2002.

[31] E. J. P. Earon, T. D. Barfoot, and G. M. T. D'Eleuterio, "Development of a multiagent robotic system with application to space exploration," in *Proc. 2001 IEEE/ASME Int. Conf. Advanced Intelligent Mechatronics Proceedings*, Como, Italy, July 2001, pp. 1267–1272.

[32] A. Isidori, *Nonlinear Control Systems*, 3rd ed. London, U.K.: Springer-Verlag, 1995, Communications and Control Engineering Series.

Joshua A. Marshall (S'01) was born in Frobisher Bay, NT, Canada. He received the B.Sc. degree in mining engineering and the M.Sc. degree in mechanical engineering from Queen's University, Kingston, ON, Canada, in 1999 and 2001, respectively. He is currently working toward the Ph.D. degree in electrical and computer engineering at the University of Toronto, Toronto, ON, Canada.

His current research interest is cooperative control systems with applications to robotics, particularly to the distributed control of autonomous vehicles.

Mireille E. Broucke (S'98–M'00) was born in Antwerp, Belgium. She received the B.S.E.E. degree in electrical engineering from the University of Texas, Austin, in 1984, and the M.S.E.E. and Ph.D. degrees from the University of California, Berkeley, in 1987 and 2000, respectively.

She has six years of industry experience at Integrated Systems, Inc., Santa Clara, CA, and several aerospace companies. From 1993 to 1996, she was a Program Manager and Researcher at California PATH, University of California, Berkeley. She is currently an Assistant Professor of Electrical and Computer Engineering at the University of Toronto, Toronto, ON, Canada. Her research interests are in hybrid systems and nonlinear and geometric control theory.

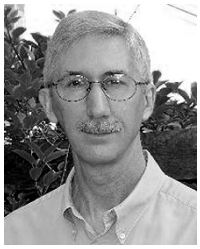

Bruce A. Francis (S'73–M'75–SM'85–F'88) was born in Toronto, ON, Canada. He received the B.A.Sc. and M.Eng. degrees in mechanical engineering and the Ph.D. degree in electrical engineering from the University of Toronto, Toronto, ON, Canada, in 1969, 1970, and 1975, respectively.

He has held teaching/research positions at the University of California, Berkeley, the University of Cambridge, Cambridge, U.K., McGill University, Montreal, QC, Canada, Yale University, New Haven, CT, and the University of Waterloo, Waterloo, ON, Canada. He is currently a Professor of Electrical and Computer Engineering at the University of Toronto.